

## 2003 Annual Report

### Interpreting focal mechanisms in a heterogeneous stress field

#### Hypothesis and Assumptions

We began to explore a new interpretation of a popular class of crustal stress analysis tools that invert focal mechanisms to determine the orientation of the principle stress axes [Gephart and Forsyth, 1984; Michael, 1987; Michael, 1991]. A critical assumption for the interpretation of this tool is that crustal stress is relatively homogeneous within spatial regions. However, spatial variations in slip in earthquakes seem to imply that crustal stress may be very heterogeneous. Furthermore, Rivera and Kanamori [2002] show that it is logically inconsistent to assume that stress is *both* homogeneous and the focal mechanisms are variable. As an alternative, we hypothesized a model which explicitly includes stress that is strongly heterogeneous. We hypothesized that the application of the traditional inversion procedure yields the orientations and relative magnitudes of the tectonic stress *rate* tensor. We suggested that this may explain why stress inversions in southern California seem to produce eigenvectors that are parallel to the strain-rate eigenvectors deduced from GPS data [Becker *et al.*, 2003].

There are two major assumptions in our procedure 1) stress is strongly spatially heterogeneous due to past earthquakes and 2) the spatially uniform (over some region) tectonic stress rate from far-field plate boundary motions brings points to failure. Hence, earthquakes are a biased sampling of those points brought closer to failure by tectonic stress. In other words, when using focal mechanisms to solve for a spatially uniform quantity, it should yield the stress rate tensor instead of the stress tensor.

#### Model of Stress in Time and Space

We assume that between the time of large earthquakes, the stress tensor can be approximately decomposed into two parts,

$$\sigma(\mathbf{x}, t) \approx \sigma_T(t)t + \sigma_R(\mathbf{x})$$

where

$\mathbf{x}$  = 3-D position

$t$  = time

and

$\sigma_T(t)$  = tectonic stress rate tensor (spatially homogeneous)

$\sigma_R(\mathbf{x})$  = spatially heterogeneous stress caused by past large earthquakes

We assume that the spatial heterogeneous part of the stress,  $\sigma_R(\mathbf{x})$ , can be modeled statistically, with perhaps a fractal distribution of stress. In addition, we assume that earthquakes nucleate when shear stress exceeds a threshold that is the same for all faults (this is consistent with laboratory observations that coefficients of friction do not vary significantly from 0.6, Byerlee's law).

In contrast, the existing paradigm for interpreting the focal mechanism inversions has the following assumptions: Short length-scale spatial heterogeneities in  $\sigma$  are small compared to the spatial average. However, a wide range of focal mechanisms are commonly observed, even within small regions. In fact, a wide range of focal mechanisms are necessary to deduce unique orientations of the stress eigenvectors when using current inversion procedures. It is commonly assumed that the fact that there are different focal mechanisms is due to a wide variation in fault friction on faults with different orientations. Specifically, Rivera and Kanamori [2002] demonstrated that one has to assume fault friction can span a wide range of values to obtain a spatially uniform stress.

#### Methodology

We have three main objectives: 1) determine how the degree of spatial heterogeneity affects the results of current stress inversion techniques, 2) compare the effects of different types of heterogeneity

(characterized by the spatial power spectrum), and 3) determine to what degree focal mechanism inversions reflect the orientation of the spatially average of the absolute stress as opposed to the orientation of the tectonic stress rate tensor.

To achieve these goals, we have the following methodology. First, generate synthetic 3-D stress fields using our new set of assumptions, i.e., stress is composed of two components, a strongly spatially heterogeneous component,  $\sigma_R(\mathbf{x})$ , and a spatially uniform tectonic stress rate,  $\dot{\sigma}_T(t)$ . To create appropriate suites of internal stress, we use a random number generator  $R(\mathbf{x})$  with a Gaussian distribution (white noise) in the three spatial dimensions to generate the five independent components of the deviatoric stress tensor. Then we use various low-pass filters to smooth the stress in space. For example, we can apply spatial filters with characteristic length scales. That is, we perform a three-dimensional running mean weighted by some spatial function, such as a Gaussian function or a rectangle function. We can also use low-pass filters that have no characteristic length scale (fractals) by fractionally integrating with respect to space. The formalism for this filtering can be expressed as follows.

$$\sigma_R(\mathbf{x}) = \mathbf{F}\mathbf{T}_{3-D}^{\square}[\mathbf{F}\mathbf{T}_{3-D}[R(\mathbf{x})]\mathbf{k}^{\square}]$$

where

$\mathbf{k}^{\square}$  is a power law filter in vector wavenumber space.

Recent theoretical work by Liu and Heaton [2003 in preparation] on the variability of slip in space on faults suggests that  $\square = 1/2$ , and this value may be compatible with actual observations of rupture vs. length scaling.

Once we have constructed a simulation of the stress tensor in space and time, we can construct an earthquake catalog by finding the locations and times at which the Hencky-Mises yield condition [Housner and Vreeland, 1965] is exceeded:

$$I_2' = \frac{2}{3}\sigma_0^2$$

where  $I_2'$ , the second invariant of the deviatoric stress tensor, is a measure of the distortional stress, and  $\sigma_0^2$  is the yield stress in uniaxial tension. Essentially, we can compute  $I_2'$  for each grid point, and determine at what time it is sufficiently large to exceed the failure stress. If the failure time is within a preselected time window, then we randomly choose one of the two possible failure planes and assign a focal mechanism to go with the event time and location. In this manner, we develop a catalog of synthetic earthquakes where the earthquakes constitute a spatially biased sample of points brought closer to failure by tectonic stress. See Figure 1, for a 1-D visualization.

We then can test the standard stress inversion techniques. We can invert each suite of synthetic focal mechanisms using two different methods, LSIB (Linear Stress Inversion with Bootstrapping) by Michaels [1987] and FMSI (Focal Mechanisms Stress Inversion) [Gephart, 1990; Gephart and Forsyth, 1984]. The terms LSIB and FMSI are borrowed from terminology used by Hardebeck [2001]. These inversions calculate four independent parameters of the deviatoric stress tensor, the three principal stress axes' orientations and a parameter that relates the relative magnitudes of the principal stresses, [Angelier, 1979]:

$$\square = \frac{\sigma_2 \sigma \sigma_3}{\sigma_1 \sigma \sigma_3}$$

where  $\sigma_1$  is the maximum principal stress,  $\sigma_2$  is the intermediate principal stress, and  $\sigma_3$  is the minimum principal stress. We take these four independent parameters for each data set and directly

compare them to their values in the original data set. We can explicitly compare the inversion results to the secular tectonic stress, the heterogeneous internal stress, as well as the summed stress. In doing so, we can determine the effect of different heterogeneities on stress inversions and how much the inversions reflect the tectonic stress rate vs. the spatial mean of the stress. Lastly, we can compare our results with real seismicity catalogs and interpret the results.

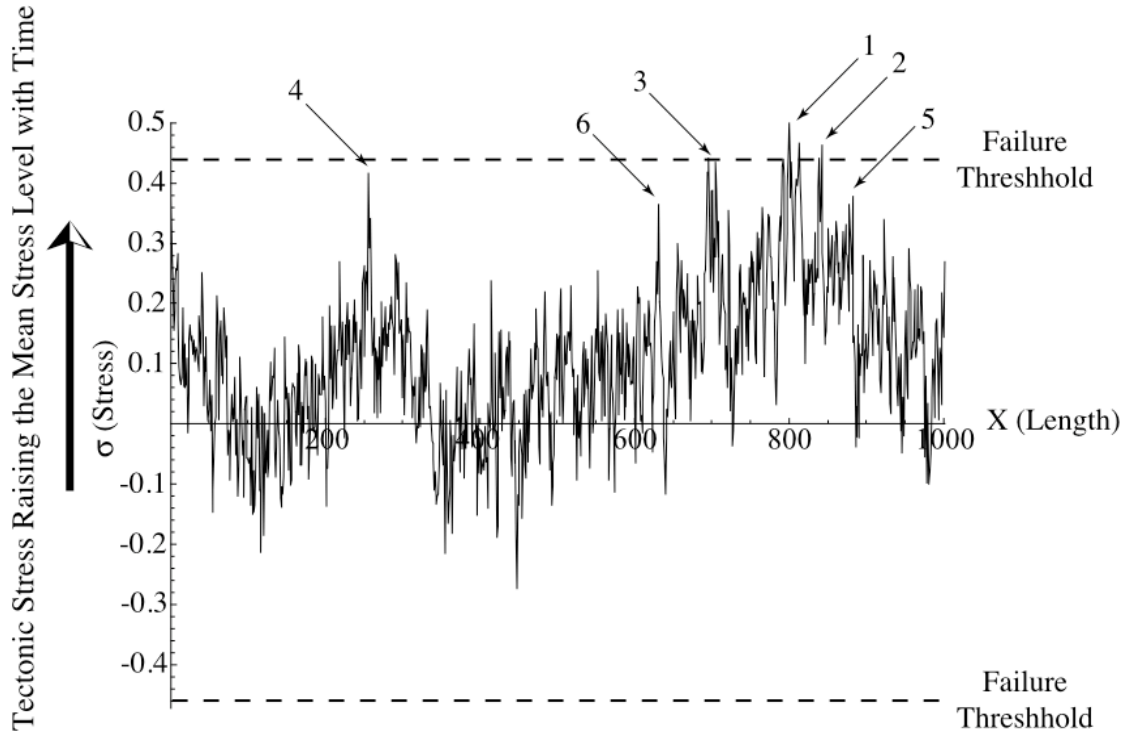


Figure 1. Internal stress is heterogeneous spatially in the direction  $X$ . In addition, there is a mean component of stress that increases as a function of time as tectonic loading is added externally. As the mean stress increases, different points along the fault cross the failure threshold and generate earthquakes. In this figure, the locations of earthquakes have been labeled in the order they would cross the failure threshold. Notice how the partially smoothed heterogeneity produces clustering of earthquakes.

### Initial Results

We have created sample 3-D stress fields as follows. Brad Aagaard's 2-D version was used as a starting point, which we expanded into 3-D.

- 1) Began with a random Gaussian distribution of stress (white noise) in three dimensions.
- 2) Convolved the distribution in the Fourier domain with our fractal filter,  $\mathbf{k}^{-\alpha}$ , where  $\mathbf{k}$  is the wave-number vector and  $\alpha$  is the filtering power.
- 3) Produced fractal stress fields on 250x250x250 point grids. Figure 1 on the left shows 2-D slices through filtered grids and on the right shows spectra of 1-D slices through the filtered grids.

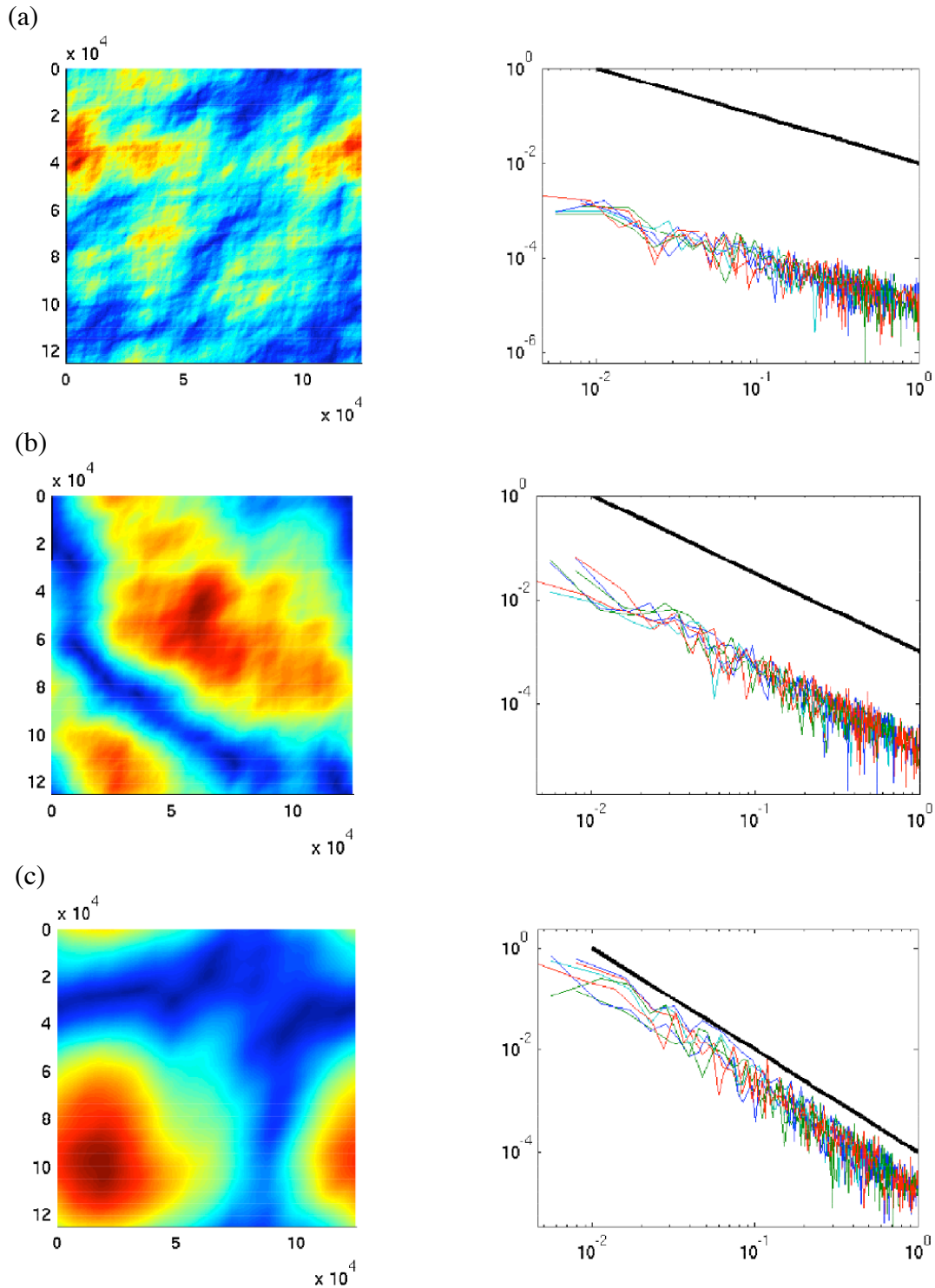


Figure 2. On the left are 2-D slices of filtered stress through the 3-D grid. On the right are the spectra of 1-D slices of filtered stress through the 3-D grid. The black lines represent the effective filtering power,  $l/l$ , used to create the 3-D grid. (a) Represents a filtering power,  $l/l = 1.0$ , (b) represents a filtering power,  $l/l = 1.5$ , and (c) represents a filtering power,  $l/l = 2.0$ .

We also have one example of an earthquake catalog that was inverted using the standard focal mechanism inversion techniques [Gephart and Forsyth, 1984; Michael, 1987; Michael, 1991]. We produced filtered 3-D grids with the five deviatoric stress components, added on a tectonic stress rate in

the horizontal plane, and solved for the time to failure using the Hencky-Mises yield condition [Housner and Vreeland, 1965]. We used an  $\lambda = 2.0$  and our stress matrix looked like this:

$$\begin{matrix} \sigma'_{xx}(x,y,z) & \sigma'_{xy}(x,y,z) + \sigma'_{xy}(\lambda)\lambda & \sigma'_{xz}(x,y,z) \\ \sigma'_{xy}(x,y,z) + \sigma'_{xy}(\lambda)\lambda & \sigma'_{yy}(x,y,z) & \sigma'_{yz}(x,y,z) \\ \sigma'_{xz}(x,y,z) & \sigma'_{yz}(x,y,z) & \sigma'_{zz}(x,y,z) \end{matrix}$$

where  $\sigma'_{xx}(x,y,z)$ ,  $\sigma'_{xy}(x,y,z)$ , etc. are the filtered random stress components of the 3-D grid and  $\sigma'_{xy}(\lambda)$  is the stress rate in the horizontal plane. If there were no filtered random heterogeneity, this matrix would produce fault planes with the following strikes, dips and rakes for maximal shear stress.

Strike	Dip	Rake
0°	90°	180°
90°	90°	0°

After determining time to failure for points within the 100x100x100 grid, we examined those points with a time to failure less than some threshold, calculated the strike, dips, and rakes for plane orientations that would yield maximal shear stress, and inverted the catalog using Andy Michael's Slick Package from the USGS quake software download site, <http://quake.wr.usgs.gov/research/software/>. This produced a stress matrix whose strikes, dips, and rakes are as follows:

Strike	Dip	Rake
≈ 0°	≈ 65°	≈ 155°
≈ 90°	≈ 65°	≈ 30°

The strikes, dips, and rakes, are close to what we would expect if the stress inversion is indeed a biased sample of points brought closer to failure by the stress rate. In other words, it is what we would expect if the stress inversion yields information about the stress rate tensor instead of the stress tensor. While this result is tentative because it needs to be followed with suites of models and different filters, it does provide additional evidence for our hypothesis.

Angelier, J., Determination of the mean principal directions of stresses for a given fault population, *Tectonophysics*, 56, T17-T26, 1979.

Becker, T.W., J.L. Hardeback, and G. Anderson, Constraints on the mechanics of the Southern San Andreas fault system from velocity and stress observations, in *Seismological Society of America Annual Meeting*, San Juan, Puerto Rico, 2003.

Gephart, J.W., FMSI: A Fortran program for inverting fault/slickenside and earthquake focal mechanism data to obtain the regional stress tensor, *Computers and Geosciences*, 16 (7), 953-989, 1990.

Gephart, J.W., and D.W. Forsyth, An improved method for determining the regional stress tensor using earthquake focal mechanism data: Application to the San Fernando earthquake sequence, *Journal of Geophysical Research*, 89 (B11), 9305-9320, 1984.

Hardeback, J.L., The crustal stress field in Southern California and its implications for fault mechanics, California Institute of Technology, Pasadena, California, 2001.

Housner, G.W., and T.J. Vreeland, *The Analysis of Stress and Deformation*, 440 pp., Division of Engineering and Applied Science, California Institute of Technology, 1965.

Liu, J., and T.H. Heaton, The effect of slip variability on earthquake slip-length scaling, 2003 in preparation.

Michael, A.J., Use of focal mechanisms to determine stress: A control study, *Journal of Geophysical Research-Solid Earth*, 92 (B1), 357-368, 1987.

Michael, A.J., Spatial variations in stress within the 1987 Whittier Narrows, California, aftershock sequence: New techniques and results, *Journal of Geophysical Research-Solid Earth*, 96 (B4), 6303-6319, 1991.